Inorg. Chem. **2006**, *45*, 10909–10921

Luminescent Hydrido-Carbonyl Clusters of Rhenium Containing Bridging 1,2-Diazine Ligands

Monica Panigati,[†] Daniela Donghi,[†] Giuseppe D'Alfonso,*[,†,§] Pierluigi Mercandelli,*[,‡,§] Angelo Sironi,[‡,§] and Laura D'Alfonso[#]

Dipartimento di Chimica Inorganica, Metallorganica e Analitica, Università di Milano and INSTM UdR di Milano, Via Venezian 21, 20133 Milano, Italy, CIMAINA, Via Celoria 16, 20133 Milano, Italy, Dipartimento di Chimica Strutturale e Stereochimica Inorganica, Università di Milano, Via Venezian 21, 20133 Milano, Italy, and Dipartimento di Fisica, Università di Milano-Bicocca, Piazza delle Scienze 6, 20126 Milano, Italy

Received August 4, 2006

The reaction of the electronically unsaturated (56 valence electrons, ve) tetrahedral cluster $[Re_4(\mu_3\text{-}H)_4(CO)_{12}]$ (**1**) with pyridazine (pydz) gives as the main initial product the tetranuclear cluster $[Re_4(\mu\text{-}H)_4(\mu\text{-}pydz)(pydz)_2(CO)_{12}]$ (**2a**), with 64 ve and four hydrogen-bridged metal–metal interactions, with a spiked-triangle geometry. One of the three pydz ligands bridges, in a cis configuration, the cluster edge opposite to the vertex bearing the spike, as indicated by the X-ray single-crystal analysis. This species slowly decomposes, affording the dinuclear unsaturated (32 ve) complex $[Re_2(\mu\text{-}H)_2(\mu\text{-}pydz)(CO)_6]$ (**3a**) and two isomers of the tetranuclear cluster $[Re_4(\mu\text{-}H)_4(\mu\text{-}pydz)_2(CO)_{12}]$ (64 ve), sharing an unusual square cluster geometry and differing in the trans (major, 85%, **4a**) or cis (**4a′**) configuration of the bridging pydz ligands. The structures of **3a** and **4a** have been ascertained by X-ray analysis, while the characterization of **4a′** was hampered by its instability (slowly transforming into **3a** in THF solution). Both the dimer and the square cluster **4a** are also formed directly (and quickly) from **1**, being present in solution since the beginning of the reaction. Cluster **4a** is the main final reaction product. The reaction with phthalazine follows a similar course, with some differences in the relative amount of the final products **3b** and **4b**. Most of the novel complexes are able to emit light in solution at room temperature, and photophysical measurements were performed in CH_2Cl_2 solution on the main stable reaction products (i.e., the dinuclear species **3a** and **3b** and the trans square clusters **4a** and **4b**). The emission was in the range of 580–645 nm, from MLCT excited states, with lifetimes on the order of a hundred nanoseconds (50–473 ns). The quantum yields were 1 order of magnitude higher for the squares (1.7 and 1.3% for **4a** and **4b**, respectively, in CH_2Cl_2) than for the dinuclear complexes (∼0.1%). In the case of **4a**, a blue shift and an increase of the emission intensity were observed upon decreasing the solvent polarity.

Introduction

A large number of electronically unsaturated hydrido-carbonyl clusters of rhenium have been synthesized and characterized in the past,[1−8] much larger than for any other transition metal. Many of these unsaturated clusters are of interest because of their peculiar reactivity, arising from the easy addition of nucleophiles. The "ethylene-like" dinuclear $[Re_2(\mu\text{-}H)_2(CO)_8]$ complex (32 valence electrons, ve), for

* To whom correspondence should be addressed. E-mail: giuseppe.dalfonso@unimi.it (G.D.); pierluigi.mercandelli@unimi.it (P.M.).
† Dipartimento di Chimica Inorganica, Metallorganica e Analitica, Università degli Studi di Milano.
‡ Dipartimento di Chimica Strutturale e Stereochimica Inorganica, Università degli Studi di Milano.
§ CIMAINA (Centro Interdisciplinare Materiali e Interfacce Nanostrutturati).
# Dipartimento di Fisica, Università degli Studi di Milano-Bicocca.

(1) Among purely hydrido-carbonyl species, we mention the dinuclear $[Re_2(\mu\text{-}H)_2(CO)_8]$ complex,[2] the trinuclear $[Re_3(\mu\text{-}H)_3(CO)_{10}]^{2-}$,[3] $[Re_3(\mu\text{-}H)_4(CO)_{10}]^-$ [4] and $[Re_3(\mu\text{-}H)_3(\mu_3\text{-}H)(CO)_9]^-$ anions (in fact the latter in the solid state has been characterized as a dimeric hexanuclear species,[5] but spectroscopic evidence suggests the monomeric trinuclear structure in solution),[6] and the tetranuclear $[Re_4(\mu_3\text{-}H)_4(CO)_{12}]$[7] and $[Re_4(\mu\text{-}H)_3(\mu_3\text{-}H)_2(CO)_{12}]^-$ species.[8]
(2) (a) Bennet, M. J.; Graham, W. A. G.; Hoyano, J. K.; Hutcheon, W. L. *J. Am. Chem. Soc.* **1972**, *94*, 6232−3. (b) Masciocchi, N.; Sironi, A.; D'Alfonso, G. *J. Am. Chem. Soc.* **1990**, *112*, 9395−7.
(3) Bertolucci, A.; Freni, M.; Romiti, P.; Ciani, G.; Sironi, A.; Albano, V. G. *J. Organomet. Chem.* **1976**, *113*, C61−4.

10.1021/ic061467z CCC: $33.50
Published on Web 12/06/2006

Scheme 1

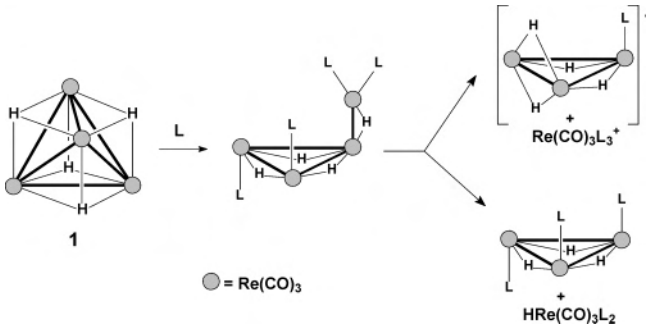

instance, provided the first example of addition polymerization of an organometallic complex that closely mimics the polymerization of olefins.[9] On the other hand, the mono- and bis-unsaturated triangular cluster anions $[Re_3(\mu\text{-}H)_4(CO)_{10}]^-$ and $[Re_3(\mu\text{-}H)_3(\mu_3\text{-}H)(CO)_9]^-$ (46 and 44 ve, respectively) provided useful platforms for anchoring organic substrates that were successively involved in hydrogen-transfer reactions.[10]

The present paper addresses novel aspects of the reactivity of the tetranuclear complex $[Re_4(\mu_3\text{-}H)_4(CO)_{12}]$ (**1**), which possesses four electrons less than that required by the effective atomic number rule (56 instead of 60 ve). In agreement with its high unsaturation, **1** reacts with any (even weakly) donor species, L.[6,7a] Surprisingly enough, however, **1** usually adds more ligands than required to attain saturation (four instead of two),[11] resulting in the formation of an unstable tetra-addition derivative with a spiked-triangle structure, which then undergoes fragmentation to lower nuclearity species, according to the two main pathways depicted in Scheme 1.[12] With weak σ-donor ligands, such as acetonitrile, tetrahydrofuran, acetone, or methanol, the reaction has the "ionic" stoichiometry 1 and affords an unsaturated (46 ve) triangular cluster anion and the $[ReL_3(CO)_3]^+$ cation.

$$[Re_4(\mu_3\text{-}H)_4(CO)_{12}] + 4L \rightarrow [Re_3(\mu\text{-}H)_4L(CO)_9]^- + [ReL_3(CO)_3]^+ \quad (1)$$

In the reaction with CO, a different (neutral) fragmentation has been observed (eq 2),[7a] while with pyridine, both the products of the ionic and of the neutral path have been identified.[12c]

$$[Re_4(\mu_3\text{-}H)_4(CO)_{12}] + 5L \rightarrow [Re_3(\mu\text{-}H)_3L_3(CO)_9] + [HReL_2(CO)_3] \quad (2)$$

In some cases, the ^1H NMR spectra of the reaction mixtures showed (besides the signals of the products of the above-described "3 + 1" fragmentations) another very minor resonance,[12b] which may be tentatively attributed to a byproduct of formula $[Re_2(\mu\text{-}H)_2L_2(CO)_6]$. Such product, which is isoelectronic to the unsaturated $[Re_2(\mu\text{-}H)_2(CO)_8]$ complex, can be assumed to arise from a "symmetric" (i.e., 2 + 2) fragmentation of the starting material **1** or of the first tetra-addition derivative. The reaction would therefore involve the transformation of the 2-fold unsaturated tetranuclear cluster **1** into two monounsaturated dinuclear complexes (eq 3).

$$[Re_4(\mu_3\text{-}H)_4(CO)_{12}] + 4L \rightarrow 2[Re_2(\mu\text{-}H)_2L_2(CO)_6] \quad (3)$$

Because of the interest in this kind of unsaturated complex, we wondered if the use of bidentate bridging ligands could favor their formation. Toward this goal, we have investigated the reactivity of **1** with 1,2-diazines because related monodentate nitrogen ligands, such as pyridines, have been found to be very effective reactants toward complex **1**.[12c] Moreover, it has already been proven that 1,2 diazines are able to act as bridging ligands on Re−H−Re interactions in hydridocarbonyl triangular rhenium clusters.[13]

By using these ligands, we have now found that the desired symmetric cleavage path (eq 3) does occur, but not selectively. Other reaction paths are also effective, affording mainly tetranuclear complexes with an unusual square geometry of the metal cage. Moreover, the novel compounds have been found to possess interesting luminescent properties, and their preliminary photophysical characterization is reported here.

Results and Discussion

The 1,2-diazines which have been used in this study are pyridazine (pydz) and phthalazine (phal), depicted in Chart 1. The reactivity of $[Re_4(\mu_3\text{-}H)_4(CO)_{12}]$ (**1**) with the two ligands was very similar, affording in both cases mixtures whose components have been unambiguously identified by joint spectroscopic (solution) and X-ray single-crystal (solid state) analysis.[14] Letters **a** and **b** have been used to label the pyridazine and phthalazine derivatives, respectively.

(4) Beringhelli, T; Ciani, G.; D'Alfonso, G.; Molinari, H; Sironi, A. *Inorg. Chem.* **1985**, *24*, 2666−71.
(5) Horng, H. C.; Cheng, C. P.; Yang, C. S.; Lee, G.-H. *Organometallics* **1996**, *15*, 2543−47.
(6) Beringhelli, T.; D'Alfonso, G. *J. Chem. Soc., Chem. Commun.* **1994**, 2631−2.
(7) (a) Saillant, R.; Barcelo, G.; Kaesz, H. *J. Am. Chem. Soc.* **1970**, *92*, 5739−41. (b) Wilson, R. D.; Bau, R. *J. Am. Chem. Soc.* **1976**, *98*, 4687−9. (c) Masciocchi, N.; D'Alfonso, G.; Kockelmann, W.; Schäfer, W; Sironi, A. *Chem. Commun.* **1997**, 1903−4.
(8) Beringhelli, T; D'Alfonso, G.; Ciani, G.; Molinari, H. *J. Chem. Soc., Chem. Commun.* **1987**, 486−8.
(9) (a) Bergamo, M.; Beringhelli, T.; D'Alfonso, G.; Mercandelli, P.; Moret, M.; Sironi, A. *J. Am. Chem. Soc.* **1998**, *120*, 2971−2. (b) D'Alfonso, G. *Chem.—Eur. J.* **2000**, *6*, 209−15.
(10) For example, see: (a) Beringhelli, T.; D'Alfonso, G.; Panigati, M.; Porta, F.; Mercandelli, P.; Moret, M.; Sironi, A. *J. Am. Chem. Soc.* **1999**, *121*, 2307−8. (b) Beringhelli, T.; D'Alfonso, G.; Panigati, M.; Mercandelli, P.; Sironi, A. *Chem.—Eur. J.* **2002**, *8*, 5340−50.
(11) Until now, evidence of the formation of a 60 ve species has been obtained only in the reaction of **1** with X^- halides. However, also in this case, the initially formed $[Re_4H_4(\mu\text{-}X)(CO)_{12}]^-$ addition derivatives, spectroscopically characterized, rapidly underwent a 3 + 1 fragmentation. Beringhelli, T; D'Alfonso, G.; Ciani, G.; Molinari, H. *J. Chem. Soc., Dalton Trans.* **1996**, 1771−3.
(12) (a) Wang, S. R.; Wang, S.-L.; Cheng, C. P.; Yang, C. S. *J. Organomet. Chem.* **1992**, *431*, 215−26. (b) Beringhelli, T.; D'Alfonso, G.; Zarini, M. *J. Chem. Soc., Dalton Trans.* **1995**, 2407−15. (c) Wang, S. R.; Cheng, C. P. *J. Organomet. Chem.* **1995**, *490*, 111−6.
(13) Beringhelli, T.; D'Alfonso, G.; Maggioni, D.; Panigati, D.; Mercandelli, P.; Sironi, A. *J. Mol. Catal. A* **2003**, *204−205*, 361−9.
(14) The spectroscopic (IR and NMR) analysis of isolated crystals confirmed the correspondence between the species observed in solution and those structurally characterized in solid.

Chart 1

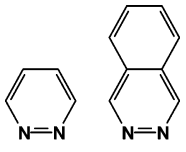

Scheme 2

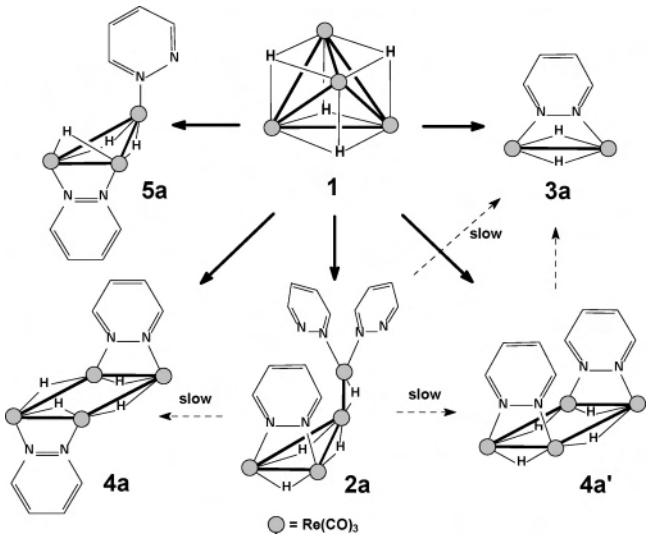

All the reactions have been performed in dichloromethane, because **1** is poorly soluble in hydrocarbons and any donor solvent (including tetrahydrofuran or acetone) causes instantaneous and complete cluster fragmentation (eq 1).[6,7]

Reaction with Pyridazine (pydz). The reaction of compound **1** with two equivalents of pydz gave an instantaneous color change from red-brown to orange, followed by the slow separation of a yellow precipitate. NMR monitoring has revealed a two-step process: the first NMR spectrum, acquired a few minutes after reagent mixing, indicated that **1** reacts almost instantaneously with pydz, giving four main products, labeled **2a**, **3a**, **4a**, and **5a** in Scheme 2, in the relative ratios reported in Figure 1. Then the composition of the reaction mixtures slowly changes because the main kinetic product **2a** converts into the thermodynamically favored species **3a** and **4a**.

The species initially present in the highest concentration is the complex $[Re_4(\mu\text{-}H)_4(\mu\text{-pydz})(pydz)_2(CO)_{12}]$, with a tetranuclear spiked-triangular metallic skeleton (**2a**, Scheme 2), accounting for slightly more than 50% of the overall intensity in the hydride region of the NMR spectra. This compound, with 64 ve and four hydrogen-bridged metal−metal interactions, is analogous to the tetra-addition derivative $[Re_4(\mu\text{-}H)_4(NCMe)_4(CO)_{12}]$ observed as the initial product in the reaction of **1** with acetonitrile.[12b] In the present case, **2a** contains three ligands only, since one of them acts as four-electron donor, by bridging the cluster edge opposite to the vertex bearing the spike and from the same side of the triangle plane as the spike (cis configuration, see Scheme 2 and Figure S1 in Supporting Information). Its three hydride resonances, in a ratio of 2:1:1 (Table 1) indicate that, in solution, the $Re(CO)_3(pydz)_2$ fragment that constitutes the spike has a (static or dynamically averaged) conformation which imparts an overall C_s symmetry to the complex. The pattern of the pyridazine resonances (six signals of intensity 2) agrees with this symmetry.

The complex **2a** has a diazine content higher than the 2:1 experimental reactant ratio. This explains the initial presence

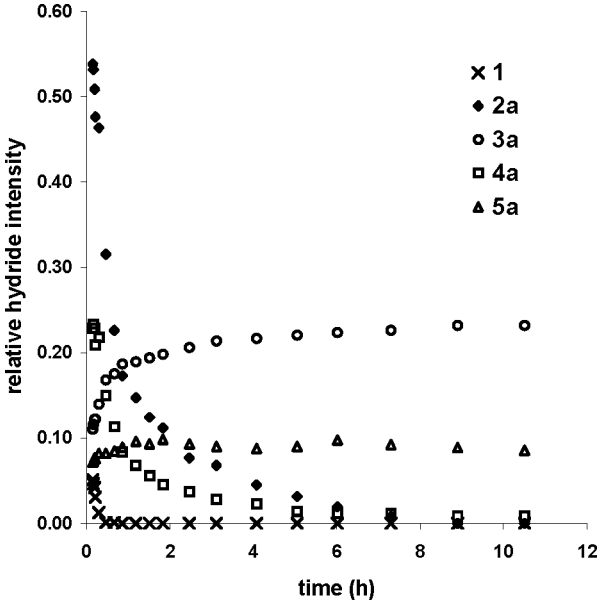

Figure 1. ^{1}H NMR monitoring of the course of the reaction of **1** with 2 equiv of pyridazine (CD_2Cl_2, 298 K). In the ordinate, the fraction of the overall hydride intensity for each species is reported.

Table 1. ^{1}H NMR Data of the Novel Complexes **2**, **3**, **4**, **4′**, and **5** (δ, CD_2Cl_2, 298 K)

	pyridazine[a]		
	H_3, H_6	H_4, H_5	hydrides
2a	9.71 (dt, 2)$_t$	7.80 (m, 2)$_t$	−10.79 (d, 2)
	9.07 (t, 2)$_b$	7.73 (m, 2)$_t$	−11.09 (s, 1)
	8.97 (dt, 2)$_t$	7.49 (t, 2)$_b$	−11.54 (t, 1)
3a	9.21 (t, 2)	7.87 (t, 2)	−3.88 (s, 2)
4a	9.68 (t,4)	8.21 (t, 4)	−9.82 (t, 2)
			−12.54 (t, 2)
4a′ [b]	9.02 (t, 4)	7.63 (t, 4)	−10.51 (t, 2)
			−11.17 (t, 2)
5a	9.47 (dd,1)$_t$	7.63 (t, 2)$_b$	−9.85 (s, 2)
	9.09(t, 2)$_b$	7.55 (m, 2)$_t$	−11.37 (s, 1)
	9.00 (dd, 1)$_t$		

	phthalazine[a]		
	H_3, H_8	H_4−H_7	hydrides
2b	10.09 (s, 2)	8.16−8.00 (m, 8)	−10.59 (d, 2)
	9.47 (s, 2)		−10.80 (s, 1)
	9.14 (s, 2)		−11.40 (t, 1)
3b	9.68 (s, 2)	8.21 (m, 4)	−3.95 (s, 2)
4b	9.66 (s, 4)	8.08 (m, 4)	−9.21 (t, 2)
		7.91 (m, 4)	−12.22 (t, 2)
4b′[b]	9.37 (s, 4)	7.86 (m, 4)	−9.98 (t, 2)
		7.83 (m, 4)	−10.79 (t, 2)
5b	9.52 (s, 2)$_b$	8.12 (m, 4)	−9.78 (s, 2)
	9.93 (s, 1)$_t$	8.03 (m,4)	−11.16 (s, 1)
	9.33 (s, 1)$_t$		
5b′	9.67 (s, 1)$_t$	8.52−8.36 (m, 8)	−8.94 (s, 2)
	9.02 (s, 2)$_b$		−10.88 (s, 1)
	8.61 (s, 1)$_t$		

[a] For compounds **2** and **5**, the subscripts b and t indicate protons belonging to the bridging and terminal diazine ligands, respectively. [b] Data in THF-d_8 solution.

of some unreacted **1**, which rapidly disappeared (see Figure 1), by consumption of the pydz released by the conversion of **2a** to species with a lower diazine/rhenium ratio (see below). When 3 equiv of pydz (i.e., the stoichiometric amount required by **2a**) was used, the initial relative amount of **2a** was higher (~70%), no unreacted **1** was observed, and significant concentrations of the same byproducts depicted in Figure S2 in the Supporting Information were formed. Interestingly, **2a** was the main initial product even when only 1 equiv diazine was used (obviously in this case the amount of unreacted **1** was much higher).

Complex **2a** is unstable in solution and slowly decomposes (Figures 1 and S2) to give **3a** (which remained in solution) and **4a** (which progressively precipitated), as discussed below.

The species labeled **3a** is the dinuclear complex $[Re_2(\mu\text{-}H)_2(\mu\text{-pydz})(CO)_6]$ (Scheme 2). As shown in Figure 1, it was present in solution since the very beginning of the reaction: actually, it is the unsaturated complex expected from the 2 + 2 fragmentation of the tetranuclear starting compound **1**, according to eq 3. The concentration of **3a** progressively increased, even after the complete disappearance of **1**, showing that it originates also from the spiked-triangular cluster **2a** (eq 4).

$$[Re_4(\mu\text{-}H)_4(\mu\text{-pydz})(pydz)_2(CO)_{12}] \rightarrow 2[Re_2(\mu\text{-}H)_2(\mu\text{-pydz})(CO)_6] + pydz \quad (4)$$

The formulation of **3a** was suggested by the chemical shift of its hydride resonance (−3.88 ppm)[15,16] and then confirmed by an X-ray single-crystal analysis (Figure S3 in Supporting Information).

The other important reaction product is the tetranuclear cluster $[Re_4(\mu\text{-}H)_4(\mu\text{-pydz})_2(CO)_{12}]$ (**4a**), isoelectronic with **2a**, but with a square geometry of the Re(μ-H)Re skeleton (see Scheme 2). It is responsible for two hydride and two pydz resonances, in the ratio of 1:1:2:2, respectively (Table 1), and an X-ray crystal analysis showed that the two pydz molecules are bridging on two opposite edges of the square, in a trans position with respect to the plane of the cluster (Figure S4 in Supporting Information).

This complex is poorly soluble in CH_2Cl_2, so that it was the main constituent of the yellow precipitate that progressively slowly separated from the reaction mixtures (85% from NMR analysis of the precipitate dissolved in THF-d_8).

The only other species present in the precipitate (representing the remaining 15% of the precipitate, from the NMR analysis) can be reasonably formulated as the isomer of **4a** in which the two pyridazine ligands are coordinated in a cis position (**4a′**, Scheme 2). The formulation is based on the close resemblance of the ^{1}H NMR data of **4a** and **4a′**, in terms of number and relative intensities of the signals (Table 1). The ^{1}H relaxation times, T_1, which are usually reliable probes of the molecular size, larger molecules having larger correlation times and shorter T_1, are also very similar. Indeed the hydrides of **4a′** had T_1 values (0.58(0.05) and 0.55(0.06) s) much closer to those of **4a** (0.41(0.01) and 0.55(0.01) s) than to that of binuclear **3a** (1.08(0.02) s). Further characterization of this very minor species was hampered by its instability, because in solvents in which it is (moderately) soluble, such as THF, it slowly underwent clean cleavage to the binuclear complex **3a**.

In spite of the insolubility in CD_2Cl_2 of the square complexes **4**, the resonances of **4a** were clearly observable in the ^{1}H NMR spectra acquired at the early reaction stages (those of **4a′** were hardly recognizable because of their much smaller concentration). This means that initially the solution was oversaturated with respect to **4a**, possibly because of the slowness of the nucleation process. Consequently, the plot of Figure 1 might be misleading with regard to the overall yield of **4a**: it depicts the slow decrease in solution because of precipitation, but when the solid phase is also taken into account, the overall amount of **4a** actually increased.

The precipitation of the two **4** isomers caused a progressive decrease of the overall hydride intensity: at the end of the reaction this "missing" intensity, evaluated by an internal standard, figured up to more than 60%. In agreement with this, when the reaction was performed on a preparative scale, the *isolated* yields of **4a** were ~50%, confirming that **4a** is the main reaction product.

Formally, **4a** is a dimer of **3a**. However, it has not been possible to transform the binuclear complex into the square cluster by refluxing in inert solvents. Irradiation of a suspension of **4a** in THF with the pyrex-filtered UV light of a mercury lamp afforded a dark solution in which the main (and the only identified) hydride species was **3a**. The reaction is reminiscent of the previously reported photochemical transformation of the square cluster $[Re_4(\mu\text{-}H)_4(CO)_{16}]$ into the unsaturated binuclear complex $[Re_2(\mu\text{-}H)_2(CO)_8]$.[17]

Since the very beginning of the reaction, the NMR spectra revealed the presence of other minor byproducts. Among these, the most important was the species **5a** (~10%), responsible for two hydride resonances (ratio 2:1), which we formulate[18] as the triangular cluster $[Re_3(\mu\text{-}H)_3(\mu\text{-pydz})(pydz)(CO)_9]$, depicted in Scheme 2. This species could be classified as a $[Re_3(\mu\text{-}H)_3L_3(CO)_9]$ derivative, arising from the 3 + 1 *neutral* fragmentation of **1** (see eq 2). In this case, however, we do not have evidence of the formation of the mononuclear complex $HRe(CO)_3(pydz)_2$, which should accompany **5a**, according to the stoichiometry of eq 2. We can assume that the bridging nature of the diazine favors the formation of the dinuclear complex **3a** rather than the monuclear $HRe(CO)_3(pydz)_2$, according to overall stoichiometry 5.

(15) The hydric signal of the isoelectronic complex $[Re_2(\mu\text{-}H)_2(CO)_8]$ is at −9.0 ppm and according to the empirical rules established for hydrido-carbonyl clusters of rhenium;[12b,16] a down-field shift of about 5 ppm is expected upon replacement of two carbonyls by two N-donor ligands.

(16) Beringhelli, T.; D'Alfonso, G.; Freni, M.; Ciani, G.; Moret, M.; Sironi, A. *J. Chem. Soc., Dalton Trans* **1989**, 1143−8.

(17) Bergamo, M.; Beringhelli, T.; D'Alfonso, G.; Garavaglia, L.; Mercandelli, P.; Moret, M.; Sironi, A. *J. Cluster Sci.* **2001**, *12*, 223−242.

(18) To confirm this formulation, we have prepared both the pydz and phal derivatives **5** by reaction of $[Re_3(\mu\text{-}H)_3(\mu_3\text{-}H)(CO)_9]^-$ with HBF_4 in the presence of 2 equiv of the proper diazine. A full characterization of these species and a study of their properties are in progress.

$$2[Re_4(\mu_3\text{-}H)_4(CO)_{12}] + 5pydz \rightarrow 2[Re_3(\mu\text{-}H)_3(\mu\text{-}pydz)(pydz)(CO)_9] + [Re_2(\mu\text{-}H)_2(\mu\text{-}pydz)(CO)_6] \quad (5)$$

The concentration of **5a** remained constant during the decomposition of **2a**, showing that the formation of **5a** from the spiked-triangle **2a** is negligible.

Reaction with Phthalazine (phal). The reaction of **1** with phthalazine was performed in the same manner as that with pyridazine. Also in this case, the addition of 2 equiv of ligand to a CH_2Cl_2 solution of **1** caused a change of the solution color (from red-brown to yellow) and the progressive separation of a yellow precipitate. NMR monitoring (Figure 2) revealed that the reaction processes, although somewhat slower, led to mixtures analogous to those observed for pydz.

The main initial product was again the spiked-triangular species (**2b**) that slowly decomposed to give the binuclear unsaturated complex **3b** and the two square clusters **4b** and **4b′**. Complex **3b** was much more insoluble in CH_2Cl_2 than **3a**, so that it was found not only in the solution but also in the precipitate:[19] a NMR analysis of the precipitate isolated after .∼20 h, dissolved in THF-d_8, showed the following composition: **3b**, 48.5; **4b**, 45.5; **4b′**, 6.0%. Moreover, in this case, two isomers of the triangular cluster (**5b** and **5b′**) have been observed (Table 1), differing in the relative coordination (cis or trans) of the bridging and terminal phal ligands.[18] Anyway, their overall hydride intensity remained always very small (<10%, Figure 2).

Solid-State Characterization. The molecular structure of the main species obtained from the reaction of the tetrahedral cluster $[Re_4(\mu_3\text{-}H)_4(CO)_{12}]$ (**1**) with pyridazine (pydz) and phthalazine (phal) was determined by X-ray diffraction analysis. The following compounds were characterized: the spiked-triangular clusters $[Re_4(\mu\text{-}H)_4(\mu\text{-diazine})(diazine)_2(CO)_{12}]$ (**2a** and **2b**), the dimeric species $[Re_2(\mu\text{-}H)_2(\mu\text{-diazine})(CO)_6]$ (**3a** and **3b**), and the square clusters $[Re_4(\mu\text{-}H)_4(\mu\text{-diazine})_2(CO)_{12}]$ (**4a** and **4b**).

ORTEP drawings of the phthalazine derivatives **2b**, **3b**, and **4b** are reported in Figures 3−5, respectively. A representation of the related pyridazine derivatives **2a**, **3a**, and **4a** can be found in the Supporting Information. Tables 2−4 contain some relevant bond lengths and angles for the dimeric species (**3a** and **3b**), the spiked-triangular clusters (**2a** and **2b**), and the square clusters (**4a** and **4b**), respectively.

In all compounds, neglecting direct metal−metal interactions, each rhenium atom attains a distorted octahedral coordination and bears three terminal carbonyl ligands with facial coordination, as in the parent tetrahedral cluster $[Re_4(\mu_3\text{-}H)_4(CO)_{12}]$. In addition, in the dimeric and square species, all rhenium atoms coordinate two hydrido ligands and a nitrogen atom of a bridging diazine-κN:N' ligand. In the spiked-triangular species, the two basal rhenium atoms Re(1) and Re(2) show this same substitution pattern, while the apical atom Re(3) bears three hydrido ligands, and the spike atom Re(4) bears a hydrido ligand and two nitrogen atoms of two terminally bound diazine-κN ligands.

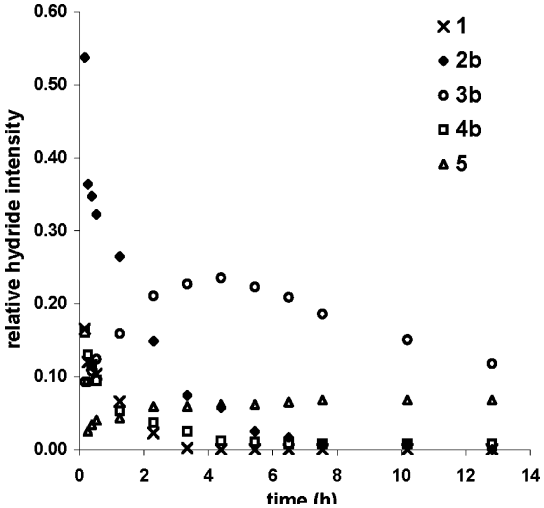

Figure 2. ^1H NMR monitoring of the course of the reaction of **1** with 2 equiv of phthalazine (CD_2Cl_2, 298 K). In the ordinate, the fraction of the overall hydride intensity for each species (for the triangular clusters it is reported as the sum of the relative hydride intensities of **5b** and **5b′**) is reported.

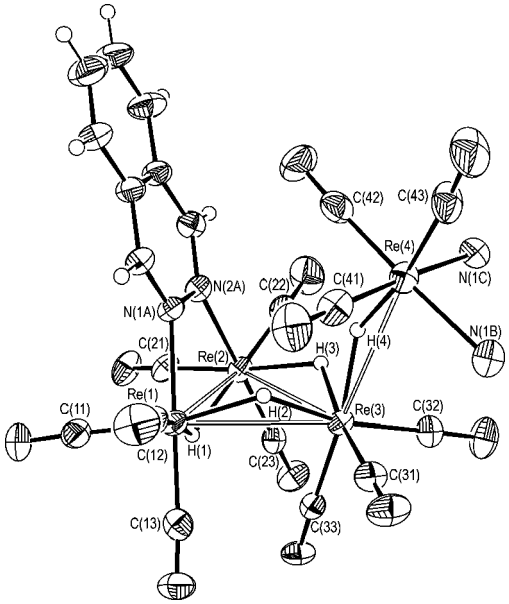

Figure 3. ORTEP drawing of the spiked-triangular cluster $[Re_4(\mu\text{-}H)_4(\mu\text{-phal})(phal)_2(CO)_{12}]$ (**2b**) showing a partial atom-numbering scheme. Thermal ellipsoids are drawn at the 30% probability level. Hydrogen atoms are given arbitrary radii. For the sake of clarity, only the metal coordinated nitrogen atoms of the phthalazine ligands bound to Re(4) are represented.

All the diazine ligands are planar, the maximum deviation from their least-squares planes being 0.06 Å. The C−N and N−N bond lengths of the heterocyclic ligands, both bridging and terminally coordinated, do not deviate significantly from the values found in the corresponding free molecules.[20] Mean Re−N bond lengths are 2.183 Å for the bridging ligands and 2.209 Å for the terminal ligands. Some of the bridging

(19) The progressive slow decrease of the relative intensity of the hydride signal of **3b** at longer times, shown in Figure 2, suggests that at intermediate times the solution was oversaturated with respect to **3b**, most likely because of the slowness of the nucleation process, as it occurs for the square clusters.

(20) (a) Blake, A. J.; Rankin, D. W. H. *Acta Crystallogr., Sect. C: Cryst. Struct. Commun.* **1991**, *47*, 1933−6. (b) Huiszoo, C.; van De Waal, B. W.; van Egmond, A. B.; Harkema, S. *Acta Crystallogr., Sect. B: Struct. Sci.* **1972**, *28*, 3415−9.

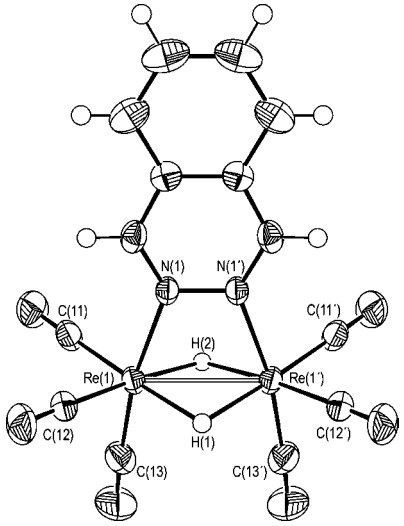

Figure 4. ORTEP drawing of the dimeric species $[Re_2(\mu\text{-}H)_2(\mu\text{-phal})(CO)_6]$ (**3b**) showing a partial atom-numbering scheme. Thermal ellipsoids are drawn at the 30% probability level. Hydrogen atoms are given arbitrary radii.

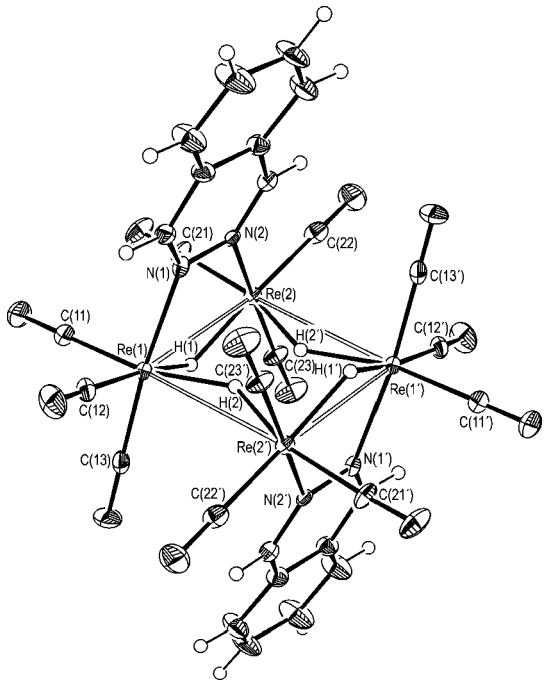

Figure 5. ORTEP drawing of the square cluster $[Re_4(\mu\text{-}H)_4(\mu\text{-phal})_2(CO)_{12}]$ (**4b**) showing a partial atom-numbering scheme. Thermal ellipsoids are drawn at the 30% probability level. Hydrogen atoms are given arbitrary radii.

diazine ligands are significantly tilted out of the ReNNRe plane. This effect is larger for the phthalazine derivatives; in particular, the tilt angle between the phthalazine least-squares plane and the ReNNRe plane in the square cluster **4b** is as large as 12.3°. This kind of distortion has been previously observed in other μ-phthalazine derivatives.[21] In compounds **2b**, **3b**, and **4b**, it can be attributed to packing interactions since no exceptional *intramolecular* nonbonded interactions can be recognized.

Table 2. Selected Bond Lengths (Å) and Angles (deg) for the Dinuclear Species $[Re_2(\mu\text{-}H)_2(\mu\text{-diazine})(CO)_6]$ **3a** and **3b**[a]

	3a	**3b**
Re(1)−Re(1')	2.8270(12)	2.7961(6)
Re(1)−C(11)	1.914(8)	1.924(5)
Re(1)−C(12)	1.934(8)	1.929(5)
Re(1)−C(13)	1.876(8)	1.916(5)
Re(1)−N(1)	2.185(5)	2.171(3)
Re(1')−Re(1)−C(11)	128.2(2)	135.56(13)
Re(1')−Re(1)−C(12)	140.8(2)	133.34(13)
Re(1')−Re(1)−C(13)	101.3(3)	99.03(15)
Re(1')−Re(1)−N(1)	69.60(15)	71.13(8)
C(11)−Re(1)−C(12)	87.5(3)	88.91(19)
C(11)−Re(1)−C(13)	91.6(4)	91.9(2)
C(11)−Re(1)−N(1)	94.8(3)	93.93(15)
C(12)−Re(1)−C(13)	92.1(3)	91.10(19)
C(12)−Re(1)−N(1)	94.7(3)	97.18(15)
C(13)−Re(1)−N(1)	170.9(3)	169.95(17)

[a] Primes refer to symmetry-equivalent atoms: x, $1/2 - y$, z for **3a** and $1 - x$, y, z for **3b**.

The carbonyl ligands are linear, with Re−C−O angles between 174.2 and 179.5°. Mean Re−C bond distances are 1.924 Å for carbonyls trans to a μ-hydrido ligand and 1.916 Å for carbonyls trans to the nitrogen atom of a diazine ligand.

The dimeric species $[Re_2(\mu\text{-}H)_2(\mu\text{-diazine})(CO)_6]$ (**3a** and **3b**) show a crystallographically imposed C_i symmetry, but if the aforementioned tilting of the diazine ligand (2.2° in **3a** and 6.7° in **3b**) is ignored, their idealized symmetry is C_{2v}. These species can be formally derived from the unsaturated compound $[Re_2(\mu\text{-}H)_2(CO)_8]$[2] by replacing two axial carbonyls with a bridging exobidentate diazine ligand.

As a consequence of the small bite of the diazine ligands, the rhenium octahedra in **3a** and **3b** are tilted with respect to $[Re_2(\mu\text{-}H)_2(CO)_8]$. The tilting can be recognized via comparison of the Re−Re−C_{ax} bond angles measured in **3a** and **3b** (101.3 and 99.0°) to the mean value observed in $[Re_2(\mu\text{-}H)_2(CO)_8]$ (92.1°). Furthermore, in **3a** and **3b**, the angles between the equatorial planes of the two rhenium atoms (each one defined by the metal atom, the two hydrides, and the two equatorial carbonyls) are equal to 26.2 and 22.1°, respectively, while in $[Re_2(\mu\text{-}H)_2(CO)_8]$, the two planes are almost coincident, in accordance with the idealized D_{2h} symmetry of this species. As a further consequence of the small bite of the diazine ligands, the Re−Re bond lengths in **3a** and **3b** (2.827 and 2.796 Å) are shorter than in $[Re_2(\mu\text{-}H)_2(CO)_8]$ (2.876 Å). The only $[Re_2(\mu\text{-}H)_2(\mu\text{-X})(CO)_6]$ species previously characterized in the solid state contains a bridging bis(diphenylphosphino)methane ligand (dppm).[22] This ligand, having a large bite comparable to that of a typical Re−Re unsaturated bond length, does not induce in the dimeric species the tilting of the rhenium octahedra and the shortening of the Re−Re bond length observed in **3a** and **3b**.[23]

The square clusters $[Re_4(\mu\text{-}H)_4(\mu\text{-diazine})_2(CO)_{12}]$ **4a** and **4b** show a crystallographically imposed C_i symmetry, but

(21) (a) Hausmann, J.; Klingele, M. H.; Lozan, V.; Steinfeld, G.; Siebert, D.; Journaux, Y.; Girerd, J. J.; Kersting, B. *Chem.—Eur. J.* **2004**, *10*, 1716−28. (b) Whitcomb, D. R.; Rogers, R. D. *Inorg. Chim. Acta* **1997**, *256*, 263−7.

(22) Prest, D. W.; Mays, M. J.; Raithby, P. R.; Orpen, A. G. *J. Chem. Soc., Dalton Trans.* **1982**, 737−45.

(23) In $[Re_2(\mu\text{-}H)_2(\mu\text{-dppm})(CO)_6]$, the Re−Re−$C_{ax}$ mean angle is 90.3°; the angle between the rhenium equatorial planes is 9.6°, and the Re−Re bond length is 2.894 Å.

Table 3. Selected Bond Lengths (Å) and Angles (deg) for the Spiked-Triangular Clusters $[Re_4(\mu\text{-H})_4(\mu\text{-diazine})(diazine)_2(CO)_{12}]$ **2a** and **2b**

	2a	**2b**		**2a**	**2b**
Re(1)−Re(2)	3.1437(8)	3.1915(5)	Re(2)−C(23)	1.914(10)	1.925(6)
Re(1)−Re(3)	3.2034(8)	3.1899(8)	Re(2)−N(2A)	2.177(7)	2.188(5)
Re(2)−Re(3)	3.2238(11)	3.2069(4)	Re(3)−C(31)	1.907(12)	1.921(6)
Re(3)−Re(4)	3.4512(10)	3.4433(8)	Re(3)−C(32)	1.917(11)	1.903(6)
Re(1)−C(11)	1.925(11)	1.933(7)	Re(3)−C(33)	1.898(10)	1.941(7)
Re(1)−C(12)	1.911(10)	1.929(6)	Re(4)−C(41)	1.908(11)	1.923(8)
Re(1)−C(13)	1.944(11)	1.916(7)	Re(4)−C(42)	1.923(11)	1.900(9)
Re(1)−N(1A)	2.183(7)	2.183(5)	Re(4)−C(43)	1.914(11)	1.914(8)
Re(2)−C(21)	1.931(10)	1.930(7)	Re(4)−N(1B)	2.206(8)	2.214(5)
Re(2)−C(22)	1.922(11)	1.911(7)	Re(4)−N(1C)	2.212(7)	2.202(5)
Re(2)−Re(1)−Re(3)	61.04(2)	60.337(13)	C(22)−Re(2)−C(23)	89.3(4)	87.6(3)
Re(1)−Re(2)−Re(3)	60.393(19)	59.806(16)	C(22)−Re(2)−N(2A)	89.5(4)	93.6(2)
Re(1)−Re(3)−Re(2)	58.566(11)	59.857(13)	C(23)−Re(2)−N(2A)	176.0(3)	178.8(2)
Re(1)−Re(3)−Re(4)	110.635(18)	104.22(2)	Re(1)−Re(3)−C(31)	103.2(4)	98.4(2)
Re(2)−Re(3)−Re(4)	113.16(2)	109.990(14)	Re(1)−Re(3)−C(32)	158.8(3)	163.94(17)
Re(2)−Re(1)−C(11)	158.6(3)	104.04(19)	Re(1)−Re(3)−C(33)	80.6(3)	78.24(17)
Re(2)−Re(1)−C(12)	97.1(3)	155.6(2)	Re(2)−Re(3)−C(31)	159.4(4)	156.6(2)
Re(2)−Re(1)−C(13)	111.4(3)	112.85(17)	Re(2)−Re(3)−C(32)	102.0(3)	107.85(17)
Re(2)−Re(1)−N(1A)	65.60(19)	65.72(12)	Re(2)−Re(3)−C(33)	80.9(3)	76.65(17)
Re(3)−Re(1)−C(11)	115.6(3)	160.38(19)	Re(4)−Re(3)−C(31)	80.9(3)	82.21(19)
Re(3)−Re(1)−C(12)	154.6(3)	108.0(2)	Re(4)−Re(3)−C(32)	83.8(3)	89.47(19)
Re(3)−Re(1)−C(13)	86.6(3)	88.51(19)	Re(4)−Re(3)−C(33)	165.1(3)	173.32(17)
Re(3)−Re(1)−N(1A)	89.13(18)	90.96(12)	C(31)−Re(3)−C(32)	94.1(5)	91.7(3)
C(11)−Re(1)−C(12)	89.5(5)	90.9(3)	C(31)−Re(3)−C(33)	87.0(4)	91.3(2)
C(11)−Re(1)−C(13)	88.7(5)	87.2(3)	C(32)−Re(3)−C(33)	88.4(4)	89.1(2)
C(11)−Re(1)−N(1A)	93.8(4)	92.8(2)	Re(3)−Re(4)−C(41)	86.9(3)	84.8(2)
C(12)−Re(1)−C(13)	90.3(4)	86.7(3)	Re(3)−Re(4)−C(42)	91.3(3)	100.2(2)
C(12)−Re(1)−N(1A)	93.2(3)	94.8(2)	Re(3)−Re(4)−C(43)	174.4(3)	171.1(3)
C(13)−Re(1)−N(1A)	175.7(3)	178.5(2)	Re(3)−Re(4)−N(1B)	88.5(2)	82.26(14)
Re(1)−Re(2)−C(21)	156.9(3)	102.59(17)	Re(3)−Re(4)−N(1C)	96.48(18)	90.45(13)
Re(1)−Re(2)−C(22)	98.8(3)	155.5(2)	C(41)−Re(4)−C(42)	87.6(5)	89.3(3)
Re(1)−Re(2)−C(23)	110.8(3)	113.84(17)	C(41)−Re(4)−C(43)	87.5(5)	91.1(3)
Re(1)−Re(2)−N(2A)	65.61(18)	65.14(12)	C(41)−Re(4)−N(1B)	89.6(4)	91.9(2)
Re(3)−Re(2)−C(21)	110.0(3)	158.13(18)	C(41)−Re(4)−N(1C)	176.2(4)	175.3(2)
Re(3)−Re(2)−C(22)	157.5(3)	111.7(2)	C(42)−Re(4)−C(43)	88.2(5)	87.6(3)
Re(3)−Re(2)−C(23)	90.5(3)	88.65(17)	C(42)−Re(4)−N(1B)	177.2(4)	177.3(3)
Re(3)−Re(2)−N(2A)	89.11(18)	91.22(11)	C(42)−Re(4)−N(1C)	90.6(3)	91.4(3)
C(21)−Re(2)−C(22)	92.5(4)	89.6(3)	C(43)−Re(4)−N(1B)	91.6(4)	90.0(3)
C(21)−Re(2)−C(23)	89.3(4)	87.3(2)	C(43)−Re(4)−N(1C)	89.1(4)	93.6(3)
C(21)−Re(2)−N(2A)	94.6(3)	92.4(2)	N(1B)−Re(4)−N(1C)	92.2(3)	87.62(19)

their geometry only marginally deviates from a C_{2h} idealized symmetry. They can be formally derived from the species $[Re_4(\mu\text{-H})_4(CO)_{16}]^{2b}$ by replacing two couples of axial carbonyls with two bridging diazine ligands. The square metal skeleton is planar, and the two diazine ligands bridge two opposite cluster edges in a trans arrangement with respect to the metal atoms' plane. The four hydrido ligands each bridge a cluster edge. Two of them lie *inside* the metal cluster, as previously observed in $[Re_4(\mu\text{-H})_4(CO)_{16}]$ and in other cyclic hydrido carbonyl rhenium clusters.[17,24]

In $[Re_4(\mu\text{-H})_4(CO)_{16}]$, the equatorial carbonyls lying next to the internal hydrido ligands show less favorable steric interactions with respect to those lying next to the external ones (mean values of the C···C contacts are 3.25 and 3.67 Å, respectively). In **4a** and **4b**, the two diazine-bridged edges Re(1)−Re(2) and Re(1′)−Re(2′) are constrained to adopt an eclipsed ligands' conformation to accommodate the small bite heterocyclic ligands. As a consequence, the internal hydrido ligands are found to bridge the other two edges of the square clusters, Re(1)−Re(2′) and Re(2)−Re(1′).

The diazine-bridged Re−Re bond lengths in **4a** and **4b** (3.190 and 3.223 Å) are shorter than that of the corresponding edges in $[Re_4(\mu\text{-H})_4(CO)_{16}]$ (3.456 Å), likewise observed for the dimeric species **3a** and **3b** with respect to $[Re_2(\mu\text{-H})_2(CO)_8]$. Bond lengths of the Re−Re edges bridged by internal hydrido ligands (3.391 and 3.420 Å) are more similar to that of the corresponding edges of $[Re_4(\mu\text{-H})_4(CO)_{16}]$ (3.422 Å).

The square clusters **4a** and **4b** can also be formally derived from the pairing of two molecules of the corresponding dimeric species **3a** and **3b**. To adopt a conformation suitable for the dimerization through the hydrido ligands, the rhenium octahedra of the $[Re_2(\mu\text{-diazine})(CO)_6]$ moiety rotate around their $(OC)_{ax}$−Re−N axes. The extent of this rotation can be ascertained by comparison of the Re(1,2)−Re(2,1)−C(21,-11) bond angles in **4a** and **4b** (95.3 and 93.4°, mean values) to the corresponding Re(1′)−Re(1)−C(11,12) bond angles in **3a** and **3b** (134.5 and 134.4°, mean values). This rotation leads to a closer interaction between the equatorial carbonyl ligands next to the diazine-bridged edges. Indeed, the C(11)···(21) nonbonded contacts in **4a** and **4b** (3.55 and 3.45 Å) are considerably shorter than the corresponding C(11,12)···C(11′,12′) contacts in **3a** and **3b** (5.51 and 5.49 Å, mean values). The proximity of the equatorial carbonyls

(24) (a) Bergamo, M.; Beringhelli, T.; D'Alfonso, G.; Mercandelli, P.; Moret, M.; Sironi, A. *Angew. Chem., Int. Ed.* **1998**, *37*, 2128−31. (b) Bergamo, M.; Beringhelli, T.; D'Alfonso, G.; Mercandelli, P.; Moret, M.; Sironi, A. *Angew. Chem., Int. Ed.* **1999**, *38*, 3486−8. (c) D'Alfonso, G.; Garavaglia, L.; Sironi, A.; Masciocchi, N. *Angew. Chem., Int. Ed.* **2000**, *39*, 4477−80.

Table 4. Selected Bond Lengths (Å) and Angles (deg) for the Square Clusters $[Re_4(\mu\text{-H})_4(\mu\text{-diazine})_2(CO)_{12}]$ **4a** and **4b**[a]

	4a	**4b**
Re(1)−Re(2)	3.1905(11)	3.2232(8)
Re(1)−Re(2')	3.3906(10)	3.4199(10)
Re(1)−C(11)	1.933(5)	1.956(6)
Re(1)−C(12)	1.934(5)	1.918(8)
Re(1)−C(13)	1.915(5)	1.935(7)
Re(1)−N(1)	2.180(4)	2.183(5)
Re(2)−C(21)	1.932(5)	1.935(8)
Re(2)−C(22)	1.925(5)	1.943(7)
Re(2)−C(23)	1.928(5)	1.895(8)
Re(2)−N(2)	2.183(4)	2.195(5)
Re(2)−Re(1)−Re(2')	89.04(3)	91.210(13)
Re(1)−Re(2)−Re(1')	90.96(2)	88.790(13)
Re(2)−Re(1)−C(11)	96.02(16)	92.6(2)
Re(2)−Re(1)−C(12)	161.25(15)	160.4(2)
Re(2)−Re(1)−C(13)	109.53(15)	110.4(2)
Re(2)−Re(1)−N(1)	65.37(10)	64.92(13)
Re(2')−Re(1)−C(11)	174.84(16)	175.7(2)
Re(2')−Re(1)−C(12)	85.27(15)	85.4(2)
Re(2')−Re(1)−C(13)	85.75(15)	86.6(2)
Re(2')−Re(1)−N(1)	88.78(11)	85.32(13)
C(11)−Re(1)−C(12)	90.2(2)	90.4(3)
C(11)−Re(1)−C(13)	91.6(2)	93.9(3)
C(11)−Re(1)−N(1)	94.23(19)	94.6(2)
C(12)−Re(1)−C(13)	87.9(2)	88.7(3)
C(12)−Re(1)−N(1)	96.61(19)	95.5(3)
C(13)−Re(1)−N(1)	172.63(17)	170.5(2)
Re(1)−Re(2)−C(21)	94.58(15)	94.1(2)
Re(1)−Re(2)−C(22)	157.71(15)	158.2(2)
Re(1)−Re(2)−C(23)	110.45(14)	113.2(2)
Re(1)−Re(2)−N(2)	64.88(11)	65.40(13)
Re(1')−Re(2)−C(21)	174.10(15)	176.8(2)
Re(1')−Re(2)−C(22)	82.83(15)	85.5(2)
Re(1')−Re(2)−C(23)	89.25(17)	87.8(2)
Re(1')−Re(2)−N(2)	87.46(11)	86.50(13)
C(21)−Re(2)−C(22)	91.3(2)	92.3(3)
C(21)−Re(2)−C(23)	90.7(2)	89.9(3)
C(21)−Re(2)−N(2)	93.03(18)	95.9(3)
C(22)−Re(2)−C(23)	90.9(2)	87.6(3)
C(22)−Re(2)−N(2)	93.38(18)	93.3(3)
C(23)−Re(2)−N(2)	174.21(18)	174.1(2)

[a] Primes refer to symmetry-equivalent atoms: $1-x, -y, -z$ for **4a** and $-x, -y, -z$ for **4b**.

pushes the hydrido ligand in between the axial carbonyls, leading to their greater separation with respect to the dimeric species. On this point, the C(13)···C(23) nonbonded contacts in **4a** and **4b** (4.51 and 4.64 Å) are longer than the corresponding C(13)···C(13′) contacts in **3a** and **3b** (3.56 and 3.40 Å).

The coupling of two $[Re_2(\mu\text{-diazine})(CO)_6]$ moieties related by a center of inversion leads to the trans isomers **4a** and **4b** of the $[Re_4(\mu\text{-H})_4(\mu\text{-diazine})_2(CO)_{12}]$ square clusters. In these species, the diazine-bridged edges adopt an eclipsed ligand conformation to accommodate the small bite heterocyclic ligands, while the remaining two edges show a sterically undemanding staggered ligand conformation.

The cis isomers **4a′** and **4b′** can be likewise obtained by coupling two $[Re_2(\mu\text{-diazine})(CO)_6]$ moieties related by a symmetry plane, leading to a structure of C_{2v} symmetry. These species should exhibit an unfavorable all-eclipsed conformation of the Re−Re edges, whose strain could be released only to some extent by relaxing the constraints of planarity of the metal skeleton. The foreseeable lower stability of the cis isomer with respect to the trans isomer is supported by its slow transformation into the dinuclear species **3** in solution.

The spiked-triangular clusters $[Re_4(\mu\text{-H})_4(\mu\text{-diazine})(\text{diazine})_2(CO)_{12}]$ **2a** and **2b** contain an isosceles triangle of rhenium atoms, Re(1)−Re(3), with a fourth metal atom bound to the apical atom Re(3), lying in the plane perpendicular to the triangle and bisecting the basal edge Re(1)−Re(2). When the conformation of the terminally coordinated diazine ligands is neglected and a small rotation of the spike fragment with respect to the Re(3)−Re(4) edge is allowed for, the molecules possess an idealized C_s symmetry, in accordance with the ^{1}H NMR evidence in solution.

At variance with the dimeric species (**3a** and **3b**) and the square clusters (**4a** and **4b**), a neutral hydrido carbonyl rhenium cluster corresponding to the spiked-triangular species **2a** and **2b** has not yet been prepared. However, clusters **2a** and **2b** can be compared to some existing derivatives of the hypothetical $[Re_3(\mu\text{-H})_3(CO)_{11}\{Re(\mu\text{-H})(CO)_5\}]$ species, namely, the iodo derivative $[Re_3(\mu\text{-H})_3(CO)_{11}\{Re(\mu\text{-H})I(CO)_4\}]^-$ and the terminal hydrido derivative $[Re_3(\mu\text{-H})_2(CO)_{11}\{Re(\mu\text{-H})H(CO)_4\}]^{2-}$ (three different polymorphs of this species have been characterized).[25] The Re(1)−Re(2) bond length (3.144 and 3.191 Å in **2a** and **2b**) is shorter then that found in the iodo derivative (3.284 Å) because of the presence of a bridging diazine ligand. In $[Re_3(\mu\text{-H})_2(CO)_{11}\{Re(\mu\text{-H})H(CO)_4\}]^{2-}$, the basal edge does not bear a bridging hydrido ligand, and the corresponding bond length (3.026 Å, mean value) is typical of a direct Re−Re interaction. The mean bond length of the lateral edges (3.214 and 3.198 Å in **2a** and **2b**, respectively) compares well to the values usually found for hydrido bridged Re−Re interactions in triangular metal clusters. The length of the spike edge Re(3)−Re(4) (3.451 and 3.443 Å in **2a** and **2b**, respectively) seems to be sensitive to the steric hindrance exerted by the ligands bound to the spike atom Re(4). Indeed, it is noticeably shortened in the iodo derivative (3.348 Å), and it is even shorter in the terminal hydrido derivative (3.287 Å, mean value).

Within the hydrido carbonyl rhenium clusters, other 64 valence-electron species have been characterized so far, namely, the aforementioned square cluster $[Re_4(\mu\text{-H})_4(CO)_{16}]$, the related $[Re_4(\mu\text{-H})_4(CO)_{16}]^-$ anion,[17] and a spiked-triangular $[Re_4(\mu\text{-H})(CO)_{17}]^-$ anion,[26] in which however the spike Re(4) occupies an equatorial position and the apical atom Re(3) shows an unusual pentagonal bipyramidal *heptacoordination* (in accordance with the presence of an additional carbonyl ligand).

The chemistry of 64 valence-electron tetranuclear clusters has attracted considerable interest because of the different skeletal topologies possible when linking four metal centers through four bonds.[27] Both square and spiked-triangular species have been identified, and the preference for one

(25) (a) Albano, V. G.; Ciani, G.; Freni, M; Romiti, P. *J. Organomet. Chem.* **1975**, *96*, 259−64. (b) Ciani, G.; Albano, V. G.; Immirzi, A. *J. Organomet. Chem.* **1976**, *121*, 237−48. (c) Ciani, G.; D'Alfonso, G.; Freni, M; Romiti, P.; Sironi, A. *J. Organomet. Chem.* **1979**, *170*, C15−7.

(26) Hillier, A. C.; Sella, A.; Elsegood, M. R. J. *J. Organomet. Chem.* **1999**, *588*, 200−4.

geometry with respect to the other has been related to the σ-donor capabilities of the ligands bound to the metal core.[28] In the present case, both geometries have been isolated. However, the two species show a different composition, since the bridging diazine ligand found in the square cluster **4a** and **4b** is replaced by two terminally bound diazine ligands in the spiked-triangular clusters **2a** and **2b**.

Whereas the pyridazine and the phthalazine derivatives of both dimers and square clusters show an identical structure, the more variable spike fragment of the spiked-triangular species **2a** and **2b** are different between the two derivatives. Indeed, in the pyridazine species **2a**, the two diazine ligands bound to the spike are oriented toward the pyridazine bridging the basal edge Re(1)−Re(2), and the ligands bound to Re(3) and Re(4) are eclipsed. In contrast, in the phthalazine derivative **2b**, the two phthalazine ligands bound to the spike are oriented away from the basal edge, and the ligands bound to Re(3) and Re(4) adopt a staggered conformation.

Luminescent Properties of the Novel Complexes. Mononuclear tricarbonyl rhenium(I) complexes containing chelating diimine ligands, of the general formula *fac*-$[Re(CO)_3(N\text{-}N)X]^{n+}$ (N-N = 1,10-phenanthroline or 2,2′-bipyridine, X = anionic or neutral monodentate ligand, with $n = 0$ or 1, respectively) have been extensively studied because of their distinctive luminescent properties.[29−34] Like other d^6 transition metal complexes, they exhibit metal-to-ligand dπ(Re)−π^*(N-N) charge-transfer absorptions (MLCT), with relatively high molar absorptivity and moderately long-lived excited states (typically 0.1−1 μs in solution at room temperature). Most of these species display intense and unstructured emission in solution, centered at about 600 nm, originating from MLCT excited terms that are mainly of triplet character (even if the large degree of spin-orbital coupling in third-row metals precludes discrete singlets and triplets).

Table 5. MLCT Absorptions and Emission Properties of the Novel Complexes **3** and **4** (CH_2Cl_2, 293 K)

	λ_{Maxabs} (nm)	ϵ ($\times 10^{-3}$)	λ_{Maxem} (nm)	ϕ ($\times 10^{2}$)	τ (ns)[a] ($f_1\ \tau_1$, $f_2\ \tau_2$)
3a	424	8.5	645	0.09	140 (0.30 450, 0.70 7.0)
3b	375 450	4.1 0.9	590	0.11	50 (0.22 190, 0.78 11)
4a	401	11.6	611	1.7	79 (0.97 81, 0.03 1.5)
4b	375[b]	21.8[b]	580	1.3	473 (0.97 488, 0.03 13)

[a] τ is the weighted average of the lifetimes, τ_i, according to their fractional intensities, f_i (see Experimental Section). [b] This absorption is a shoulder of a more intense absorption at about 330 nm attributable to an intraligand transition.

Over the past few years, many luminescent polynuclear rhenium(I) complexes have also been synthesized. They are composed of octahedral $Re(CO)_3X$ corners connected by bridging 1,4-diazines or bipyridines, leading not only to molecular squares or rectangles, typically, but also to dimers or triangles.[35−39] Such compounds bear some resemblance to the main stable products obtained here from the reaction of **1** with 1,2-diazines (i.e., the dinuclear complexes **3** and the square clusters **4**), so we performed a preliminary investigation of the photophysics of our novel species.

The absorption spectra, in addition to the bands in the range 230−330 nm that include intraligand $\pi-\pi^*$ and $n-\pi^*$ diazine transitions,[40,41] show also rather-broad lower-energy bands (with maxima in the range of 370−450 nm, see Table 5 and Figures 6 and 7) which can be assigned to MLCT transitions, by comparison with the above-discussed tricarbonyl Re(I) complexes containing diimine ligands.[29−39] Moreover, both the strong blue shift observed upon increasing solvent polarity[42,43] (see Table 6 and Figures S5 and S6 in Supporting Information) and the red-shift caused by introduction of electron-withdrawing substituents on the diazine, which makes the ligand reduction in the CT

(27) Shriver, D. F.; Kaesz, H. D.; Adams, R. D. *The Chemistry of Metal Cluster Complexes*; VCH: New York, 1990.
(28) Einstein, F. W. B.; Johnston, V. J.; Pomeroy, R. K. *Organometallics* **1990**, *9*, 2754−62.
(29) For pioneer works, see: (a) Wrighton, M.; Morse, D. L. *J. Am. Chem. Soc.* **1974**, *96*, 998−1003. (b) Giordano, P. J.; Fredericks, S. M.; Wrighton, M. S.; Morse, D. L. *J. Am. Chem. Soc.* **1978**, *100*, 2257−59. (c) Luong, J. C.; Nadjo, L.; Wrighton, M. S. *J. Am. Chem. Soc.* **1978**, *100*, 5790−95. (d) Fredericks, S. M.; Luong, J. C.; Wrighton, M. S. *J. Am. Chem. Soc.* **1979**, *101*, 7415−17. (e) Smothers, W. K.; Wrighton, M. S. *J. Am. Chem. Soc.* **1983**, *105*, 1067−69.
(30) Kalyanasundaram, K. *J. Chem. Soc., Faraday Trans. 2* **1986**, *82*, 2401−2415.
(31) (a) Caspar, J. V.; Meyer, T. J. *J. Phys. Chem.* **1983**, *87*, 952−57. (b) Caspar, J. V.; Westmoreland, T. D.; Allen, G. H.; Bradley, P. G.; Meyer, T. J.; Woodruff, W. H. *J. Am. Chem. Soc.* **1984**, *106*, 3492−3500. (c) Caspar, J. V.; Sullivan, C. B.; Meyer, T. J. *Inorg. Chem.* **1984**, *23*, 2104−2109.
(32) Juris, A.; Campagna, S.; Bidd, S.; Lehn, J.-M.; Ziessel, R. *Inorg. Chem.* **1988**, *27*, 4007−11.
(33) (a) Sacksteder, L.; Zipp, A. P.; Brown, E. A.; Streich, J.; Demas, J. N.; DeGraff, B. A. *Inorg. Chem.* **1990**, *29*, 4335−40. (b) Sacksteder, L.; Lee, M.; Demas, J. N.; DeGraff, B. A. *J. Am. Chem. Soc.* **1993**, *115*, 8230−8.
(34) (a) Lees, A. J. *Chem. Rev.* **1987**, *87*, 711−43. (b) Schanze, K. S; MacQueen, D. B.; Perkins, T. A.; Cabana, L. A. *Coord. Chem. Rev.* **1993**, *122*, 63−89. (c) Lees, A. J. *Coord. Chem. Rev.* **1998**, *177*, 3−35. (d) Stukfens, D. J.; Vlcek, A., Jr. *Coord. Chem. Rev.* **1998**, *177*, 127−79. (e) Striplin, D. R.; Crosby, G. A. *Coord. Chem. Rev.* **2001**, *211*, 163−75.
(35) Lee, S. J.; Lin, W. *J. Am. Chem. Soc.* **2002**, *124*, 4554−5.
(36) (a) Rajendran, T.; Manimaran, B.; Lee, F.-Y.; Lee, G.-H.; Peng, S.-M.; Wang, C.-M.; Lu, K.-L. *Inorg. Chem.* **2000**, *39*, 2016−7. (b) Manimaran, B.; Rajendran, T.; Lu, Y.-L.; Lee, G.-H.; Peng, S.-M.; Lu, K.-L. *Dalton Comm.* **2001**, 515−7. (c) Rajendran, T.; Manimaran, B.; Lee, F.-Y.; Chen, P-J.; Lin, S.-C.; Lee, G.-H.; Peng, S.-M.; Chen, Y.-J.; Lu, K.-L. *Dalton Trans.* **2001**, 3346−51. (d) Rajendran, T.; Manimaran, B.; Liao, R.-T.; Lin, R.-J.; Thanasekaran, P.; Lee, G.-H.; Peng, S.-M.; Liu, Y.-H.; Chang, I-J.; Rajagopal, S. *Inorg. Chem.* **2003**, *42*, 6388−94.
(37) (a) Slone, R. V.; Yoon, D. J.; Calhoun, R. M.; Hupp, J. T. *J. Am. Chem. Soc.* **1995**, *117*, 11813−4. (b) Slone, R. V.; Hupp, J. T.; Stern, C. L.; Albrecht-Schmitt, T. E. *Inorg. Chem.* **1996**, *35*, 4096−7. (c) Slone, R. V.; Hupp, J. T. *Inorg. Chem.* **1997**, *36*, 5422−5423. (d) Benkstein, K. D.; Hupp, J. T.; Stern, C. L. *Inorg. Chem.* **1998**, *37*, 5404−5. (e) Slone, R. V.; Benkstein, K. D.; Bélanger, S.; Hupp, J. T.; Guzei, I. A.; Rheingold, A. L. *Coord. Chem. Rev.* **1998**, *171*, 221−243.
(38) (a) Sun, S.-S.; Lees, A. J. *J. Am. Chem. Soc.* **2000**, *122*, 8956−67. (b) Sun, S.-S.; Lees, A. J. *Organometallics* **2002**, *21*, 39−49.
(39) Tapolsky, G.; Duesing, R.; Meyer, T. J. *Inorg. Chem.* **1990**, *29*, 2285−97.
(40) Halverson, F.; Hirt, R. C. *J. Chem. Phys.* **1951**, *19*, 711−8.
(41) Hirt, R. C.; King, F. T.; Cavagnol, J. C. *J. Chem. Phys.* **1956**, *25*, 574−6.
(42) Drago, R. S. *Physical Methods in Chemistry*; W. B. Saunders Company Ed.: Philadelphia, PA, 1977.
(43) Also, see: Giordano, P. J.; Wrighton, M. S. *J. Am. Chem. Soc.* **1979**, *101*, 2888−97 and refs therein.

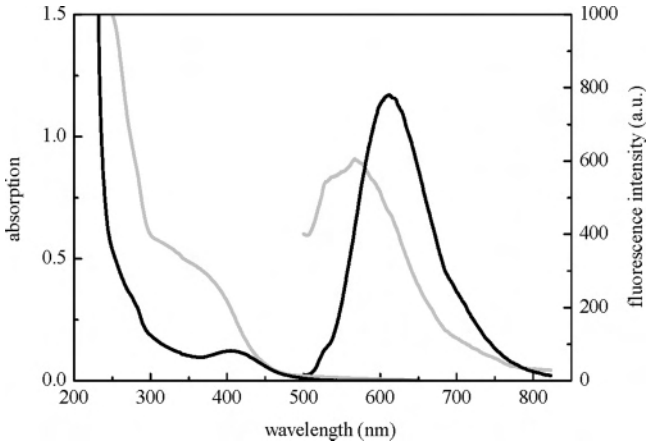

Figure 6. Absorption and emission spectra of the square clusters **4a** (black) and **4b** (gray line) in CH_2Cl_2 at 293 K. The signals at ~530 nm arise from the Raman emission of the solvent.

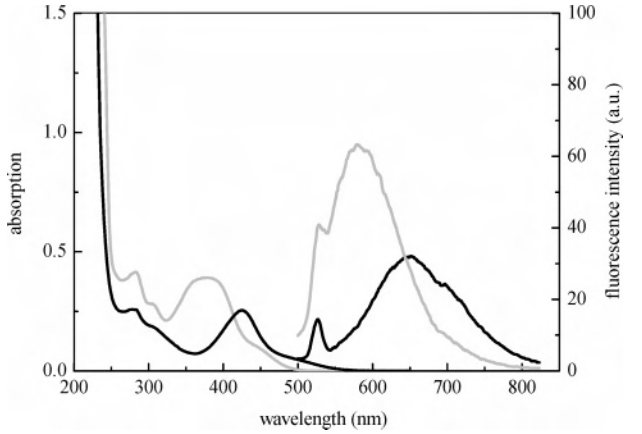

Figure 7. Absorption and emission spectra of the binuclear complexes **3a** (black) and **3b** (gray line) in CH_2Cl_2 at 293 K. The signals at ~530 nm arise from the Raman emission of the solvent.

Table 6. Solvent Effect on the Absorption Spectra of **3a** and **4a** and on the Emission Spectrum of **4a**

	3a	**4a**		
solvent	λ_{Maxabs} (nm)	λ_{Maxabs} (nm)	λ_{Maxem} (nm)	ϕ ($\times 10^2$)
acetonitrile	386	378	624	0.66
THF	402	386	612	1.3
CH_2Cl_2	424	401	611	1.7
Toluene	427	404	605	4.3
cyclohexane(5)/CH_2Cl_2(1)	448	410	571	6.8

transition easier, are typical of charge-transfer Re−L(π^*) absorptions:[29,43] indeed the absorption of the dinuclear species shifted from 425 nm for the pyridazine derivative **3a** to 470 nm for the derivative (expressly synthesized)[44] containing 3,6-Cl_2-pyridazine and to 390 nm for the phthalazine derivative **3b**.

In CH_2Cl_2 solution at 293 K, the four novel complexes emit at about 600 nm (Table 5 and Figures 6 and 7; i.e., in the same spectral region of the monomeric diimine tricarbonyl species, with a blue shift for phthalazine with respect to pyridazine). The emission arises from the lowest excited level and then, in these cases, from MLCT excited states

(44) Donghi, D.; D'Alfonso, G.; Mauro, M.; Panigati, M.; Mercandelli, P.; Sironi, A. Unpublished work.

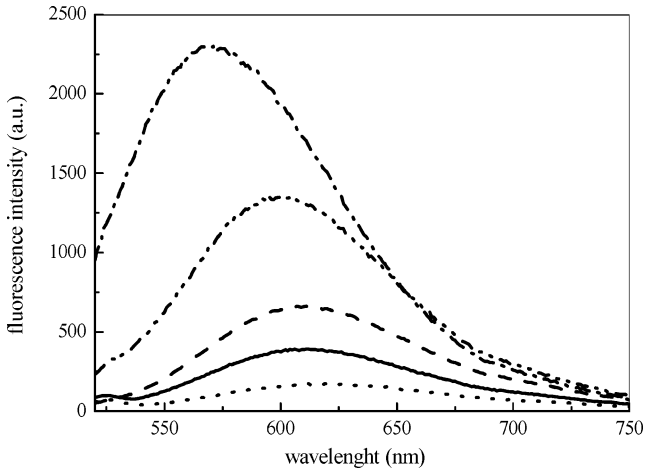

Figure 8. Emission spectra of **4a** in different solvents at 293 K: acetonitrile (· · ·), tetrahydrofuran (—), CH_2Cl_2 (- - -), toluene (-···-··), cyclohexane/CH_2Cl_2 (5/1) (-·-·).

(emission from the free ligand is very weak and occurs at much higher energy of ~420 nm).[45,46] The excitation spectra (Figure S8 in Supporting Information) above 250 nm strongly resemble the corresponding absorption spectra, indicating that emission is independent of the excitation wavelengths.

The quantum yields, measured in solution at 293 K, are about 1 order of magnitude higher for the square clusters **4** than for the dinuclear complexes **3** (Table 5).

The solvent effect has been checked for the square cluster **4a** (Table 6).[47] The emission maximum was solvent dependent, which is a characteristic of MLCT emission,[48] and showed an opposite trend with respect to what was observed for the absorption. The blue shift of the emission in the less polar solvents was accompanied by a strong increase of its intensity, as shown in Figure 8 (and Table 6). The latter behavior is in agreement with the usual increase of the rate of nonradiative decay when the emission energy decreases.[49] The red shift of the emission in polar solvents, despite a blue shift in the absorption, is typical of emission resulting from intramolecular charge transfer (that leads to dipole moment in the excited larger than in the ground state), provided that the viscosity of the solvent allows solvent relaxation in the excited-state lifetime.[50,51]

(45) All the complexes show also a weak emission at lower energy (~700 nm, Figures 6 and 7). The parent cluster **1** exhibits intense emission just at this energy, resulting from an excited state localized in the partially filled (because of the electronic unsaturation of **1**) bonding orbitals associated with the six hydrogen-bridged metal−metal bonds.[46] This possible source of emission is clearly ruled out for the square clusters, **4**, because they are electronically saturated, and therefore, transitions involving metal−metal bonding electrons are expected at much higher energy.[46] The origin of the weak emissions here observed at ~700 nm. will be investigated, also theoretically, in a future work.

(46) Graff, J. L.; Wrighton, M. S. *J. Am. Chem. Soc.* **1981**, *103*, 2225−31.

(47) In the case of **3a**, sizable effects on the position of the emission maximum and on the quantum yields could not be clearly recognized (Figure S7 in Supporting Information) possibly because of the poor emitting power of this species.

(48) (a) Shaw, J. R.; Schmehl, R. H. *J. Am. Chem. Soc.* **1991**, *113*, 389−94. (b) Wallace, L.; Rillema, D. P. *Inorg. Chem.* **1993**, *32*, 3836−43.

(49) Lacowicz, J. R. *Principles of Fluorescence Spectroscopy, II*; Kluwer: New York, 1999.

(50) Valeur, B. *Molecular Fluorescence, Principles and Applications*; Wiley-VCH: Weinheim, Germany, 2002.

The lifetimes of the excited states have been measured in the frequency domain, and the fitting of the resulting phase shifts and modulation curves required a two-exponential model for all compounds.[52] Table 5 shows the parameters of the fittings as well as the weighted averaged lifetimes. A faster decay component (lifetimes on the order of 10 ns) was dominant in the case of the dinuclear complexes (70−80%), while for the square clusters **4**, a slower component (lifetimes on the order of 100 ns) accounted for more than 97% of the relaxation. In all cases, the weighted averaged lifetimes were in the range 50−500 ns, typical for the solution room-temperature emission of Re(I) tricarbonyl complexes.

Conclusions

The results of the present study embody features of significance from different points of view.

For cluster chemistry, novel synthetic potentialities of the superunsaturated tetrahedral species $[Re_4(\mu_3\text{-}H)_4(CO)_{12}]$ (**1**) have been discovered, confirming the unique role of this molecule in the chemistry of rhenium clusters.

Although the main (unstable) kinetic product **2** of the reaction with 1,2-diazines is analogous to that formed in the reaction of **1** with monodentate donors,[12b] the final (stable) products are very different (and perhaps more valuable). In particular, no derivatives of the ionic pathway described by eq 1 were observed, and the yield of the products of the neutral 3 + 1 fragmentation was minimal. Such a deep difference between 1,2-diazines and closely related ligands such as pyridines[12c] is mainly attributable to the capability of 1,2-diazines to bridge a metal−metal interaction.

The starting idea that the use of potentially bridging ligands might favor the symmetric 2 + 2 fragmentation has been confirmed. The binuclear unsaturated complexes $[Re_2(\mu\text{-}H)_2(\mu\text{-diazine})(CO)_6]$ (**3**) so obtained are expected to exhibit high reactivity, compared with that of the other binuclear complexes containing the electron-deficient" $Re(\mu\text{-}H)_2Re$ moiety,[2,3,53] for reactions of hydrogen transfer or addition of nucleophiles. The complexes **3** originate not only from **1** but also from the fragmentation of the intermediate **2** (eq 4): this provides another example of formation in mild conditions of unsaturated derivatives from saturated intermediates.[8,11,12]

Moreover, stable derivatives with a tetrametallic skeleton have been obtained: actually, the square clusters **4** (formally dimers of **3**) are the main reaction products. Two pathways leading to their formation have been shown. The first one consists of the very unusual "direct" (i.e., without detectable intermediates) transformation of a tetrahedral cluster (**1**) into a square cluster. The second pathway involves the rearrangement of the isoelectronic spiked-triangle **2** (the kinetic product) into the thermodynamically favored square species.

Clusters with a square geometry are rare.[27] Entropic reasons, attributable to the presence of two (bridging) ligands, rather than the four ligands required for monodentate ligands, might explain the increased stability of squares species in the present case. Therefore it will be of interest to determine if the reaction of **1** with bidentate ligands provides a general synthetic method for this type of square cluster. However, the present study has shown that the composition of the reaction mixtures does not depend only on the thermodynamic stability of the products but rather results from a subtle balance of the kinetic constants ruling the different reaction paths of **1**. Therefore, even minor ligand modifications might be sufficient to change the product distribution. So the possible use of this approach for synthesizing a family of square clusters of formula $[Re_4(\mu\text{-}H)_4(\mu\text{-}LL)_2(CO)_{12}]$, with different LL bridging ligands, is far from being assured.

From the point of view of the functional properties, the synthesized products represent a novel family of polynuclear luminescent complexes of rhenium(I). The novelty is twofold, with respect to the large number of luminescent mono- and polynuclear tricarbonyl rhenium complexes containing chelating or bridging diimine ligands, which have been previously synthesized and investigated. Indeed the compounds here described represent the first luminescent tricarbonyl-diimine-rhenium derivatives exhibiting (hydrido-bridged) Re−Re interactions (even if the emission clearly originates from MLCT states rather than from metal−metal bonding orbitals, as it occurs for the parent cluster **1**).[46] Moreover, the use of 1,2-diazines as ligands in this field is unprecedented, possibly because of both the poor emitting properties of the free molecules and their rather constraining geometric requirements as ligands: indeed 1,2-diazines cannot be used as chelating ligands, like 2,2′-bipyridines, and are less amenable than isomeric 1,4-diazines to connect smaller building blocks in the assembly of polynuclear aggregates.

The emitting properties of the novel complexes, at least for the square clusters, are comparable, in terms of quantum yields and lifetimes, to those of many classical tricarbonyl-diimine-rhenium complexes. Because of the high current interest for the application of luminescent complexes in different fields, such as photonics and sensors,[54] we have now undertaken a systematic study aimed at the investigation of how changes of the cluster nuclearity of the diazine substituents and the ancillary ligands can modify the photophysical properties of this family of complexes.

(51) Baba, H.; Goodman, L.; Valenti, P. C. *J. Am. Chem. Soc.* **1966**, *88*, 5410−5.

(52) As observed by a reviewer, there are remarkably few examples in which a pure complex exhibits two lifetimes in homogeneous fluid solution at room temperature, the need for two lifetimes usually resulting from a second component. The problem of impurities is exacerbated when the main complex exhibits rather weak emission, which is the case here. Being aware of all this, we did our best to minimize the risk of spurious emission, as detailed in the Experimental Section, and the body of evidence leads us to think that the presence of an elusive luminescent impurity is less probable than a true two lifetime decay. The investigation about the molecular properties responsible for this behavior is deferred to a future work, which will be focused on the photophysics of the novel complexes.

(53) Mays, M. J.; Prest D. W.; Raithby, P. R. *J. Chem. Soc., Chem. Commun.* **1980**, 171−3.

(54) For example, see: (a) Holder, E.; Langeveld, B. M. W.; Schubert, U. S. *Adv. Mater.* **2005**, *17*, 1109−21. (b) Keefe, M. H.; Benkstein, K. D.; Hupp, J. T. *Coord. Chem. Rev.* **2000**, *205*, 201−228.

Experimental Section

All reactions were performed under N_2 using Schlenk techniques. All the solvents were deoxygenated and dried by standard methods. Pyridazine and phthalazine were purchased from Aldrich: the latter was used as received, while the former was distilled after it was kept on KOH overnight. The parent cluster $[Re_4(\mu_3\text{-}H)_4(CO)_{12}]$ was prepared according to literature procedures.[55] ^{1}H NMR spectra were recorded on Bruker DRX300 or DRX400 spectrometers. IR spectra were acquired on Bruker Vector 22 FT instrument. Electronic absorption spectra were recorded on Jasco V-570 spectrophotometer, at room temperature. Steady-state fluorescence measurements have been performed by a Cary Eclipse (Varian Inc., Australia) spectrofluorometer at constant temperature (293 K), controlled by a Peltier thermostatic system. The solutions were prepared under N_2 by introduction of the quartz cuvettes into suitable Schlenk tube, and were deoxygenated before measurements by freeze−pump−thaw cycles. Sample fluorescence has been excited at 454 nm. Emission was detected using a Hamamatsu R928 PMT. Reported spectra are not corrected for detector response. The emission intensities have been normalized to a nominal absorption value of 0.1. Quantum yields have been determined by comparison with the emission of $[Ru(bpy)_3]Cl_2$ in acetonitrile, employed as a standard ($\Phi = 0.062$).[56] Excitation spectra have been performed by fixing the emission wavelength at the main intensity peak for all the examined samples.

Dynamic fluorescence measurements have been performed with a frequency-modulated phase fluorometer (Digital K2, I.S.S., Urbana IL). The excitation was accomplished by the 30 mW output of the 454.5 nm line of an argon ion laser (2025, Spectra Physics, Mountain View, CA). At least fifteen data points at logarithmically spaced frequencies in the range of 0.3−60 MHz with a cross-correlation frequency of 80 Hz have been acquired for lifetime measurements. The convenient accuracy for phase angles and modulation ratios has been of 0.2 and 0.004°, respectively. Lifetime measurements have been performed under the magic angle conditions, and a 535 nm long pass filter (Andover Co.) has been employed to cut light scattering. A solution of glycogen in doubly distilled water has been used as reference sample.[57] Lifetime data fitting has been accomplished by an ISS routine based on the Marquardt least-squares minimization with a single- or double-exponential decay scheme. The fit of the fluorescence intensity decay $F(t)$ yields the lifetime values, τ_i, together with the corresponding fractional intensities, f_i

$$F(t) = \sum_{i=1}^{2} \alpha_i e^{-t/\tau_i} \text{ and } f_i = \alpha_i\tau_i / \sum \alpha_i\tau_i \qquad (6)$$

where α_i represents the pre-exponential factors.

To minimize the risk that the two lifetimes observed for **3a** and **3b** (see Table 5) derived from spurious emission: (i) isolated crystals were employed for the measurements, (ii) the purity of the samples was checked by NMR before and after the measurements, (iii) the possible presence of luminescent impurities in the solvent was ruled out by observing that no emission was measured in the absence of the complexes, (iv) lifetime measurements (for **3a**) were repeated in a different solvent (toluene), again two lifetimes were observed (even if with slightly different fractions: 0.8/0.2 rather than 0.7/0.3), v) lifetime measurements have also been performed using a 590 nm long pass filter, to avoid possible artifacts induced by any remaining stray light, and (vi) finally, the possibility of photogenerated emitting species was excluded by verifying that the spectra and the lifetimes of **3a** were insensitive to irradiation for about 1 h, both in CH_2Cl_2 and in toluene solution.

NMR Monitoring of the Reaction of 1 with Pyridazine. A sample of $[Re_4(\mu_3\text{-}H)_4(CO)_{12}]$ (**1**) (7.0 mg, 0.0064 mmols) was dissolved in CD_2Cl_2 (1.2 mL) directly in an NMR tube, and 10 μL of a CD_2Cl_2 solution of NEt_4BF_4 (corresponding to ∼0.0007 mmol) was added as internal standard; 2 equiv of pyridazine (45 μL of a 0.275 M CD_2Cl_2 solution, 0.0128 mmols) was added at room temperature under N_2. Then the tube was briefly shaken and introduced into the NMR probehead at 298 K. A sequence of automatic acquisition of the spectra started within 5 min of the reagent mixing. The reaction was monitored for about 12 h. In Figure 1, the fraction of the overall hydride intensity resulting from each of the species observed in solution at different times (**1**, **2a**, **3a**, **4a**, and **5a**) is reported. The corresponding NMR data are reported in Table 1.

NMR Monitoring of the Reaction of 1 with Phthalazine. The procedure was the same as above: a sample of **1** (6.7 mg, 0.0062 mmols) dissolved in 1.2 mL of CD_2Cl_2 was treated with 2 equiv of phthalazine (72 μL of a 0.166 M CD_2Cl_2 solution, 0.0120 mmols). The reaction course was monitored for about 12 h (Figure 2). The spectroscopic data of **2b**, **3b**, **4b**, **5b** and **5b′** are reported in Table 1.

Synthesis of the Pyridazine Derivatives 3a and 4a. A solution of **1** (71.6 mg, 0.0577 mmol) in CH_2Cl_2 (10 mL) was treated at room temperature with 2 equiv of freshly distilled pyridazine (8.5 μL, 0.1154 mmol). The color of the solution changed progressively from red-brown to orange and after a few minutes a yellow precipitate began to separate. The solution was stirred overnight; then the precipitate was separated by filtration from the orange solution. The solution was concentrated and treated with *n*-hexane, causing the precipitation of pure **3a** as a brick red powder. Isolated Yield: 11.7 mg (0.019 mmol, 16.3%). Elemental Anal. Calcd for **3a**: C, 19.29; H, 0.97; N, 4.50. Found: C, 19.40; H, 0.98; N, 4.59. The composition of the yellow precipitate (41 mg) was determined by ^{1}H NMR spectrum in THF-d_8 solution. It contained only the isomers **4a** and **4a′** in a ratio of 5.6:1. The complete conversion of **4a′** into **3a** was performed by stirring a suspension of the square complexes **4** in THF for 1 day at room temperature. Then the solution was evaporated to dryness, and the residue was treated with CH_2Cl_2 to extract the dinuclear compound **3a**. The yellow residue, insoluble in CH_2Cl_2 and containing the isomer **4a** only, was dissolved in THF and precipitated by addition of *n*-hexane. Isolated Yield: 34.8 mg (0.028 mmol, 48.4%). Elemental Anal. Calcd for **4a**: C, 19.29; H, 0.97; N, 4.50. Found: C, 19.37; H, 0.93; N, 4.45. IR (CH_2Cl_2) ν(CO) for **3a**: 2042 m, 2014vs, 1941s(sh), 1927s, cm^{-1}. IR (acetone) ν(CO) for **4a**: 2020vs, 1928s, cm^{-1}. IR (acetone) **4a′**: 2048 m, 2022vs, 1951 m, 1920w, cm^{-1} (the latter data have been obtained by spectral subtraction from the mixture of the square complexes **4a** + **4a′**).

Synthesis of the Phthalazine Derivatives 3b and 4b. A solution of **1** (40.6 mg, 0.0327 mmol) in CH_2Cl_2 (10 mL) was treated at room temperature with two equivalents of phthalazine (400 μL, 0.065 mmols, of a CH_2Cl_2 solution 0.16 M). The color of the solution changed instantaneously to yellow, and after few minutes, the formation of a yellow precipitate was observed. The solution was stirred overnight, and the precipitate was separated from the pale yellow solution. The composition of the precipitate was determined by NMR analysis in THF-d_8: **3b**, 48.5; **4b**, 45.5; **4b′**,

(55) (a) Andrews, M. A.; Kirtley, S. W.; Kaesz, H. D. *Inorg. Chem.* **1977**, *16*, 1556−61. (b) Johnson, J. R. Kaesz, H. D. *Inorg. Synth.* **1978**, *18*, 60−2.
(56) Caspar, J. V.; Meyer, T. J. *J. Am. Chem. Soc.* **1983**, *105*, 5583−90.
(57) For further details, see: Collini, M.; Chirico, G.; Baldini, G.; Bianchi, M. E. *Biopolymers* **1995**, *53*, 227−39.

6.0% (in mol). The precipitate (31.6 mg) was suspended in THF (10 mL) at room temperature for about 1 day to convert **4b′** into **3b**, and then it was evaporated to dryness. The residue was suspended in CH_2Cl_2 (80 mL), and the solid, composed of the tetranuclear cluster **4b**, was collected via suction filtration, washed with CH_2Cl_2, dissolved in THF, and precipitated with *n*-hexane. Isolated Yield: 15.2 mg (34%). Elemental Anal. Calcd for **4b**: C, 25.00; H, 1.20; N, 4.16. Found: C, 25.50; H, 1.20; N, 4.13. This indicates that the dried powder of **4b** does not contain CH_2Cl_2, but instead, it was found to be clathrated in the crystals. The filtrates, mainly containing the binuclear compound **3b**, were collected and purified by column chromatography on Florisil using a 3:1 CH_2Cl_2/*n*-hexane mixture as eluent. The product was precipitated by the addition of *n*-hexane to a CH_2Cl_2 solution (isolated yield 9.4 mg, 0.014 mmol, 21%). Elemental Anal. Calcd for **3b**: C, 25.00; H, 1.20; N, 4.16. Found: C, 25.05; H, 1.35; N, 3.98. IR (CH_2Cl_2) ν(CO) for **3b**: 2039 m, 2013vs, 1938s, 1923s, cm^{-1}. IR (THF) ν(CO) for **4b**: 2017s, 1924s, cm^{-1}.

Isolation of Crystals Suitable for X-ray Analysis. Crystals of **2a** were obtained from a CH_2Cl_2 solution of **1**, treated at 273 K with 2 equiv of pyridazine and maintained at 248 K for a few days. Single crystals of **3a** were obtained by slow diffusion of *n*-hexane vapors into a CH_2Cl_2 solution of isolated **3a** at 248 K. Single crystals of **4a** were obtained by slow diffusion of *n*-hexane into a THF solution of isolated **4a** at 248 K. Crystals of **2b**, **3b**, and **4b** were grown at room temperature from a concentrated CH_2Cl_2 solution of **1** treated with 2 equiv of phthalazine. IR (CH_2Cl_2) ν(CO) for **2a**: 2043m, 2025s, 2016vs, 2004m, 1927s(br) cm^{-1}. IR (CH_2Cl_2) ν(CO) for **2b**: 2040m, 2023s, 2013vs, 2001m, 1924s(br) cm^{-1}.

T_1 Measurements of 3a, 4a, and 4a′ in THF-d_8. A THF-d_8 solution of a mixture of **4a** and **4a′**, partially converted into **3a**, was accurately deoxygenated (by freeze−pump−thaw cycles). T_1 measurements were carried out at room temperature using the standard inversion recovery pulse sequence, on a Bruker DRX instrument, operating at 300 MHz.

X-ray Diffraction Structural Analysis. Data for **2a**·CH_2Cl_2: $C_{25}H_{18}Cl_2N_6O_{12}Re_4$, M = 1410.15, monoclinic, $P2_1/n$ (No. 14), a = 10.244(3) Å, b = 35.857(9) Å, c = 10.438(3) Å, β = 110.29(2)°, V = 3596.2(17) Å^3, Z = 4, D_x = 2.605 g cm^{-3}, λ(Mo Kα) = 0.71073 Å, μ = 13.633 mm^{-1}, F(000) = 2560, T = 295(2) K, $R(F)$ = 0.0296, $R_w(F^2)$ = 0.0802.

Data for **2b**·$3CH_2Cl_2$: $C_{39}H_{28}Cl_6N_6O_{12}Re_4$, M = 1730.17, monoclinic, $C2/c$ (No. 15), a = 38.445(5) Å, b = 13.365(2) Å, c = 24.569(3) Å, β = 128.62(2)°, V = 9863(4) Å^3, Z = 8, D_x = 2.330 g cm^{-3}, λ(Mo Kα) = 0.71073 Å, μ = 10.175 mm^{-1}, F(000) = 6416, T = 295(2) K, $R(F)$ = 0.0256, $R_w(F^2)$ = 0.0609.

Data for **3a**: $C_{10}H_6N_2O_6Re_2$, M = 622.56, monoclinic, $P2_1/m$ (No. 11), a = 5.675(2) Å, b = 15.810(6) Å, c = 7.963(3) Å, β = 98.94(2)°, V = 705.8(5) Å^3, Z = 2, D_x = 2.930 g cm^{-3}, λ(Mo Kα) = 0.71073 Å, μ = 17.159 mm^{-1}, F(000) = 556, T = 295(2) K, $R(F)$ = 0.0244, $R_w(F^2)$ = 0.0609.

Data for **3b**: $C_{14}H_8N_2O_6Re_2$, M = 672.62, orthorhombic, *Cmca* (No. 64), a = 15.577(3) Å, b = 16.197(3) Å, c = 12.805(3) Å, V = 3230.7(11) Å^3, Z = 8, D_x = 2.766 g cm^{-3}, λ(Mo Kα) = 0.71073 Å, μ = 15.006 mm^{-1}, F(000) = 2432, T = 295(2) K, $R(F)$ = 0.0236, $R_w(F^2)$ = 0.0497.

Data for **4a**: $C_{20}H_{12}N_4O_{12}Re_4$, M = 1245.18, monoclinic, $P2_1/c$ (No. 14), a = 8.354(4) Å, b = 16.312(8) Å, c = 10.512(5) Å, β = 109.04(2)°, V = 1354.1(11) Å^3, Z = 2, D_x = 3.054 g cm^{-3}, λ(Mo Kα) = 0.71073 Å, μ = 17.887 mm^{-1}, F(000) = 1112, T = 90(2) K, $R(F)$ = 0.0169, $R_w(F^2)$ = 0.0425.

Data for **4b**·CH_2Cl_2: $C_{29}H_{18}Cl_2N_4O_{12}Re_4$, M = 1430.18, monoclinic, $P2_1/n$ (No. 14), a = 10.858(3) Å, b = 9.760(3) Å, c = 17.527(5) Å, β = 98.84(2)°, V = 1835.3(9) Å^3, Z = 2, D_x = 2.588 g cm^{-3}, λ(Mo Kα) = 0.71073 Å, μ = 13.356 mm^{-1}, F(000) = 1300, T = 295(2) K, $R(F)$ = 0.0335, $R_w(F^2)$ = 0.0750.

R factors are defined as $R(F) = \sum||F_o| - |F_c||/\sum|F_o|$ and $R_w(F^2) = [\sum w(F_o^2 - F_c^2)^2/\sum wF_o^4]^{1/2}$. A thorough description of data collection, structure solution, and structure refinement can be found in the Supporting Informatio.

Acknowledgment. We thank the Italian MIUR for financial support (COFIN 2003, Metal Carbonyl Clusters Functional to Nanomaterials; FIRB 2003, Molecular compounds and hybrid nanostructured material with resonant and non resonant optical properties for photonic devices) and the Italian CNR (ISTM) for providing facilities for inert atmosphere and low-temperature experiments. Finally, we want to thank an anonymous reviewer who provided useful suggestions for improving the photophysical characterization.

Supporting Information Available: Eight figures showing ORTEP drawings of the pyridazine derivatives **2a**, **3a**, **4a**, the time course of the reaction of **1** with 3 equiv of pydz, the solvent effects on the photophysics of **3a** and **4a**, the excitation spectra of **3a**, **3b**, **4a**, **4b**, the crystallographic data in CIF format. This material is available free of charge via the Internet at http://pubs.acs.org.

IC061467Z